Self-Assembly of Collagen-Mimetic Peptide Amphiphiles into Biofunctional Nanofiber

Jingnan Luo[†] and Yen Wah Tong[†,‡,*]

[†]Department of Chemical and Biomolecular Engineering, National University of Singapore, 4 Engineering Drive 4, Singapore 117576, and [‡]Division of Bioengineering, National University of Singapore, 4 Engineering Drive 4, Singapore 117576

ABSTRACT Molecular assembly of protein and peptide is highly specific and frequently occurs in biological systems. Collagen, which is the most abundant component in extracellular matrix, can assemble into fiber and play an essential role in cell adhesion and growth. Since native collagen is difficult to modify and can engender pathogenic and immunological side effects, its application on tissue regeneration is limited. The preparation of collagen-mimetic materials, hence, is gaining interest in the field of tissue regeneration. Collagen peptides have been synthesized to mimic some properties of collagen, such as its triple helix. However, few studies have been done to prepare artificial collagen fiber to mimic its high-level structure and biofunctions. In this work, a novel collagen-mimetic peptide amphiphile (CPA) was prepared by conjugating a single hydrophobic tail with a collagen-mimetic peptide, supplemented with bioactive glycine-phenylalanine-hydroxyproline-glycine-glutamate-arginine (GFOGER). The physical studies indicated that the CPA had a collagen-mimetic triple-helical conformation and was able to self-assemble into nanofiber. In addition, the CPA conjugated with the integrin-specific GFOGER sequence was shown to promote collagen-mimetic cell adhesion and development. The self-assembled peptide nanofiber was shown to have the ability to structurally and biologically mimic native collagen fiber. We anticipate that this artificial collagen fiber holds great potential as collagen-mimetic materials for tissue regeneration applications.

KEYWORDS: self-assembly · peptide nanofiber · triple helix · collagen · cell adhesion

Biomolecules have the remarkable ability to self-assemble into well-defined and intricate structures.[1] One of the most typical examples is collagen, the most prevalent component in extracellular matrix.[2] Collagen molecules consist of three polypeptide α chains, each of them containing a repeating Gly-Xxx-Yyy sequence, where X and Y are usually proline and hydroxyporline.[3,4] The three chains are supercoiled around a central axis to form a triple helix, which is the fundamental and characteristic structural unit of collagen. Essential biophysical properties of collagen are derived from the triple helix, including thermal stability, mechanical strength, and the ability to engage in specific interactions with other biomolecules.[2] Collagen fibrillogenesis, the assembly of collagen into fibers *in vivo*, is mainly due to this triple-helix structure. On the other hand, the collagen fibrillogenesis has a stabilizing effect on the triple helix. *In vivo*, collagen molecules are synthesized by cells and released out into the extracellular space after intracellular enzymatic modification. In the extracellular space, collagen molecules assemble to form fibers to support cell development and tissue formation. Collagen fibers are of broad biomedical importance and have a central role in arthritis, tissue repair, fibrosis, tumor invasion, and cardiovascular disease.[2,5,6] Collagens are thought not only as structural constituents in extracellular matrix but also as functional biomolecules. Some cell-binding motifs, such as aspartic-glycine-glutamate-alanine (DGEA) and GFOGER, were found in collagen. Several integrins, such as $\alpha_1\beta_1$, $\alpha_2\beta_1$, $\alpha_3\beta_1$, $\alpha_{10}\beta_1$, and $\alpha_{11}\beta_1$, have been shown to bind to these bioactive motifs of collagen and activate cytoplasmic intracellular signaling pathways.[7−11] Integrin-mediated cell adhesion to collagen is known to be crucial for biological processes such as embryogenesis, homeostasis, and tissue remodeling and healing.[12,13]

Much progress has been made in elucidating and mimicking the structure of the collagen triple helix and its stability.[2] Synthetic collagen model peptides comprising the repeating units of glycine-proline-hydroxyproline (GPO) have been synthesized and used to study the triple helix of collagen. The stability of the triple helix was dependent on the number of repeating units. In addition, collagen-mimetic peptides containing unnatural residues have also been synthesized, including repeating Gly-Nleu-Pro, Gly-Pro-Nleu, and Gly-Pro-FPro (where Nleu = *N*-isobutylglycine, FPro = *trans*-4-fluoroproline).[14−16] These collagen peptides with unnatural residues have been shown to enhance the stability of the triple helix. Recently, bioactive motifs

* Address correspondence to chetyw@nus.edu.sg.

Received for review January 11, 2011 and accepted September 7, 2011.

Published online September 07, 2011
10.1021/nn202822f

were introduced to make these peptides biofunctional. The integrin-specific GFOGER sequence, derived from residues 502−507 of collagen α_1 (I), has been identified as a major cell-binding site within type I collagen.[17−20] Different from other collagen cell-binding motifs, GFOGER within the triple-helical domain of collagen is recognized by integrin receptors in a conformation-dependent manner. Previously, we have synthesized collagen-mimetic peptides (CMPs) by incorporating GFOGER into the repeating structural units $(GPO)_n$.[19−21] The CMP sequence was designed as GPOGPOGPOGPOGFOGERGPOGPOGPOGPOGPO, which has been shown to form a triple helix and possess collagen-mimetic functions such as cell adhesion, and has been used to engineer collagen-mimetic bioactive surfaces.[19,21−23]

These synthetic collagen-mimetic peptides mentioned above, although valuable for understanding and mimicking the triple-helix structure and functional properties of collagen, are limited for many potential biomaterial applications. The limitation is mainly due to their small size, which does not approach the scale of natural collagen protein or fiber. Inspired by collagen biosynthesis, material scientists thus are seeking to fabricate artificial collagen fibers that can resemble the properties of natural collagen fibers *via* chemical and self-assembly routes. Raines' group and Koide's group have independently designed and synthesized short collagen fragments in which the three strands are held in a staggered array by disulfide bonds.[24,25] Self-assembly of these short, triple-helix fragments was mediated by the association of the sticky ends, resulting in collagen fibers as long as 400 nm.[24] Maryanoff and co-workers developed a π-stacking approach to produce micrometer-scale triple-helical fiber.[26] Przybyla and Chmielewski used metal-induced self-assembly to obtain collagen fibers.[27] Recently, Chaikof and co-workers reported the observation of a *D*-periodic structure in their synthetic collagen fibers.[28] All of these have successfully fabricated artificial collagen fibers with some properties of native collagen, which have narrowed the gap in biophysical properties between native and artificial collagen fibers. However, more work is necessary to bridge this gap, especially for incorporating biological properties. The fabrication of artificial collagen fibers with both structural and biofunctional properties may provide significant potential applications in tissue regeneration.

In this work, we aim to use a self-assembly strategy of single-tail peptide amphiphiles to scale up collagen-mimetic peptides to form artificial collagen fibers with both the structural and biological properties of native collagen. This molecular self-assembly strategy was developed by Stupp's group and has been shown to be a versatile way for simultaneously controlling nanostructure and chemical functionality.[29−32] Briefly, CMPs were synthesized and conjugated into single hydrophobic carbon tails to form CPAs. The nanostructure and chemical functionality of self-assembling CPAs were then studied through various characterization methods. Transmission electron microscopy (TEM) was used to study the self-assembled nanostructure of CPAs. The conformation of CPAs was characterized using circular dichroism (CD) spectroscopy and melting curve analysis. Cell-binding activity of CPAs was studied through cell adhesion and cytoskeletal immunofluorescence staining. These studies may provide a better understanding of the fabrication of artificial collagen fibers using a single-tail peptide amphiphile strategy, and the fabricated collagen-mimetic fibers should hold high potential for tissue regeneration applications.

RESULTS AND DISCUSSION

Design and Synthesis of Collagen-Mimetic Peptide Amphiphiles. A series of CPAs have been designed and synthesized, based on the designing principles of single-tail peptide amphiphiles.[30−34] CPAs contain four segments, namely, an N-terminal palmityl segment, a β-sheet-forming segment, a lysine spacer, and an epitope segment, shown in Figure 1. The single palmityl segment is designed to drive amphiphilic molecules to aggregate into micelles. The β-sheet segment aims to elongate the micelles into nanofibers *via* β-sheet-type hydrogen binding. The lysine spacer is used to connect the epitope segment with hydrophobic and beta-sheet segments as well as to make CPAs controllable. In this work, three collagen-mimetic peptide sequences were inserted into the epitope segments of peptide amphiphiles, as shown in Table 1. Collagen-mimetic peptide 1 (CMP1) incorporated with the GFOGER motif, $(GPO)_3GFOGER(GPO)_3$, has been found to form a triple helix and possess biofunctions such as promoting liver cell adhesion, proliferation, and functions in previous studies.[19−21] CPA composed of CMP1 in the epitope segment is termed CPA1, as shown in Figure 1. In addition, two reference CPAs (*i.e.*, CPA2 and CPA3) were designed and synthesized. The difference between CPA2 and CPA1 is the absence of the bioactive sequence GOFGER. In CPA3, a short collagen-mimetic peptide, $(GPO)_2GFOGERGPO$, was inserted in the epitope segment. All peptide sequences were synthesized by the solid phase peptide synthesis method and then were conjugated with palmitic acid *via* an amide bond to form peptide amphiphiles. Mass spectroscopy was used to verify the identity of each product, and the result showed that the molecular weight of each product obtained was consistent with that of the desired product.

Although peptide amphiphiles incorporated with small bioactive sequences such as arginine-glycine-aspartic acid (RGD) and isoleucine-lysine-valine-alanine-valine (IKVAV) in epitope segments have been shown to self-assemble into nanofibers and have

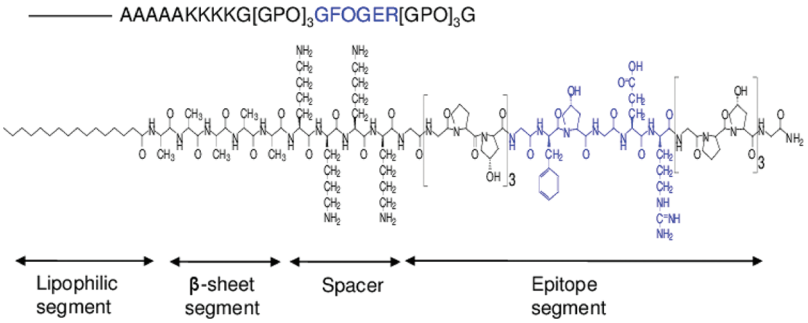

Figure 1. Molecular structure of CPA1 that contains four segments: lipophilic, β-sheet, spacer, and epitope segments. A bioactive GFOGER sequence is inserted within the repeating structural unit GPO as the epitope segment.

TABLE 1. Primary Molecular Sequence of CPAs and Their Molecular Weights

CPA	sequence[a]	molecular weight
CPA1	C16-AAAAAKKKKG(GPO)$_3$**GFOGER**(GPO)$_3$G	3502.1
CPA2	C16-AAAAAKKKKG(GPO)$_8$G	3376.9
CPA3	C16-AAAAAKKKKG(GPO)$_2$**GFOGER**GPOG	2572.0

[a] Standard one-letter code is used to express the amino acid sequences, except where noted. O represents a hydroproline residue.

corresponding biofunctions,[34,35] it is unknown whether CPAs incorporated with long collagen peptides in epitope segments could self-assemble into nanofiber. Fields' and Tirrell's groups, for example, have synthesized collagen peptide amphiphiles by conjugating collagen peptides with single or double hydrocarbon tails.[36] However, their collagen peptide amphiphiles have formed only spherical micelles instead of nanofibers.[36−39] Moreover, even if CPAs could self-assemble into well-defined nanofibers, it is still unknown whether the collagen-mimetic peptide segments could form a triple helix and retain biofunctions in the formation of nanofibers. The process of the self-assembly of CPAs is hypothesized and shown in Figure 2. It is hypothesized that the CPAs may form triple helices in aqueous solution and may self-assemble into nanofibers after screening the positive charges of the lysine spacer. To confirm this hypothesized self-assembly process and to verify the biofunctions of self-assembled nanofibers, studies of nanofiber morphology, secondary structure, and cell assay were performed.

Study of Morphological Structure. Amphiphilic molecules can spontaneously form micelles in aqueous solution when the concentration is above a critical micelle concentration (CMC). The CMC of CPAs is around 0.003 mg/mL. Thus, the subsequent experiments were conducted above this concentration to ensure micellization. TEM micrographs of Figure 3 show the morphology of self-assembled CPA1 after screening the positive charges of the lysine spacer *via* base induction of NH_4OH. The micrographs indicate that, after screening the positive charges in the lysine spacer, the CPA1 can self-assemble into nanofibers with a diameter of approximately 16 nm and lengths in the micrometer range. CPA2 and CPA3 can also self-assemble into nanofibers with similar morphology when their charges are similarly screened (see Figure S1 in the Supporting Information). The diameter of the CPA3 fiber, around 13 nm, is slightly smaller than that of CPA1 and CPA2, which may be due to its shorter head group. On the basis of the TEM micrographs, the absence of a triple helix in CPA3 does not obviously affect the morphological properties of the self-assembling nanofibers. In addition, we observed that CPAs could also self-assemble into nanofibers, although short, without screening the positive charges. The above results demonstrate that CPAs incorporated even with long collagen-mimetic peptides can self-assemble into nanofibers instead of spherical micelles, which is not consistent with the results from previous studies of Fields' group.[36,37,40,41] The self-assembly of collagen peptide amphiphiles synthesized by Fields' group into spherical micelles instead of nanofibers may be due to the presence of hydroxyproline in the β-sheet segment, because hydroxyproline has been shown to disrupt the formation of β-sheet-type hydrogen bonding. In our design, the AAAAA sequence is introduced next to the single-hydrocarbon tail to be a β-sheet segment, in which the β-sheet-type hydrogen bonding is formed to drive the elongation of micelles into nanofibers. In addition, peptide nanofiber hydrogels can form when the concentration of CPAs is increased and the charges are screened, as shown in Figure 4. To visualize its structure, the hydrogel was treated by the critical point drying technique and was observed using scanning electron microscopy (SEM). SEM micrographs of Figure 4c show the fiber-network structure of the hydrogel. The formation of the hydrogel may be due to the entanglement of nanofibers. The peptide fiber hydrogel holds high potential for the application of tissue engineering and regeneration.

CD Spectra. Structurally, native collagen has a triple-helix characteristic. To mimic native collagen, the formation of the triple helix thus is inevitable and is fundamental, which greatly affects the biophysical properties of collagen, such as thermal stability, molecular assembly, and bioactivity. The collagen-mimetic triple helix exhibits a unique CD spectrum

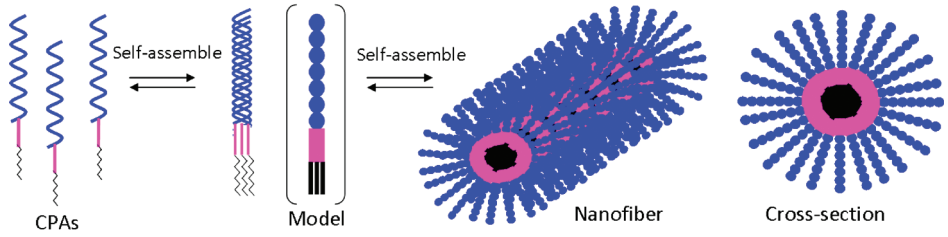

Figure 2. CPA1 self-assembly process: three collagen-mimetic peptide head groups self-assemble into a triple helix, while the hydrophobic tails and β-sheet-type hydrogen bonding drive and guide the assembly of triple-helical CPA1 into nanofibers. The peptide portion is exposed on the periphery of the nanofiber.

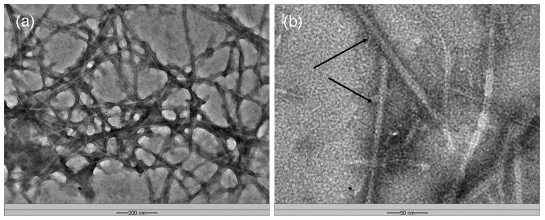

Figure 3. TEM micrographs of self-assembled peptide nanofibers with a diameter of ~16 nm. The peptide concentration for TEM testing was 0.1 mg/mL, which was diluted from 1% w/v peptide gel.

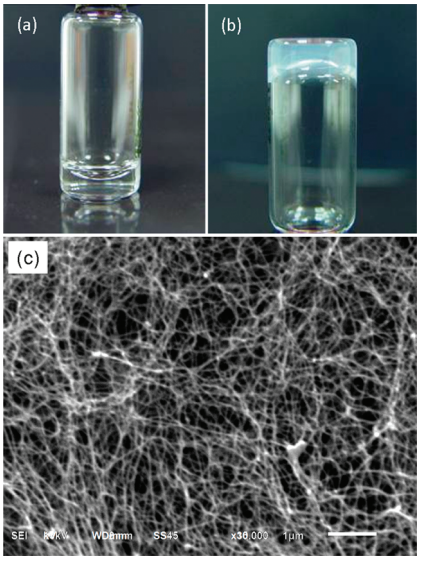

Figure 4. CPA solution (a) with 1% w/v concentration was prepared in deionized water and treated with NH_4OH to screen the positive charges to form peptide nanofiber gels (b). The vial was tipped upside down to illustrate that the gel is self-supporting. (c) SEM image of the peptide gel after critical point drying.

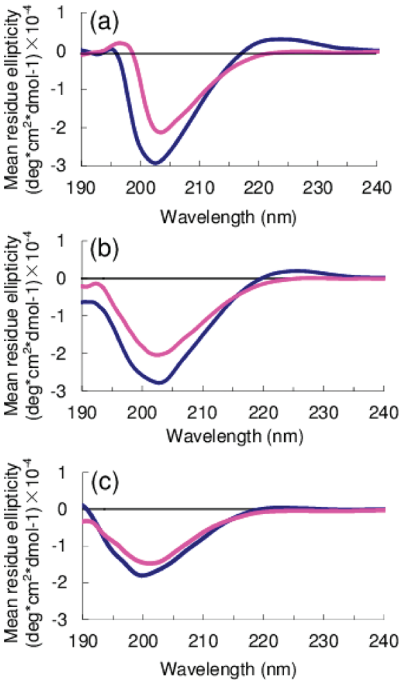

Figure 5. CD spectra of (a) CPA1, (b) CPA2, and (c) CPA3 obtained at room temperature (blue line) and 70 °C (pink line). Samples were prepared at 0.5 mg/mL in water.

characterized by a positive peak at around 220 nm, a crossover near 213 nm, and a large negative peak at approximately 197 nm (see Figure S2 in the Supporting Information).[42,43] The CD spectra of CPA1, CPA2, and CPA3 at 25 and 70 °C are shown in Figure 5. CPA1 exhibited CD spectral features characteristic of a collagen-mimetic triple helix, with a positive peak around 220–225 nm and a large negative one near 200 nm, as shown in Figure 5a. The CD spectra of CPA1 displayed a red shift in band positions with respect to the CD spectral band positions of collagen, probably due to the higher percentage of amino acid content.[44] Similar to native collagen, the temperature can affect the peak intensity of CPA1: at higher temperature, the peak has lower intensity. In the CD spectra of CPA2, similar trends were observed, indicating the presence of a triple helix. In addition, the CD spectra of CPA3 did not display any feature that is indicative of the presence of a triple helix. The absence of a triple helix in CPA3 may be because there are not enough repeating structural units of $(GPO)_n$ to drive the folding of CPA3 into the triple-helix structure. The above results demonstrate that CPA1 and CPA2 may have triple-helix secondary structure, but CPA3 should not display the feature of a collagen-mimetic triple helix.

Melting Point Study. Since the CD spectrum of the collagen-mimetic triple helix is similar to that of the Polypro II helix, further verification of the formation of

the triple helix in CPAs is necessary. Triple helices melt in a highly cooperative manner, as the structures are stabilized by both intra- and interstrand hydrogen-bonding water networks.[45−47] This provides a basis for distinguishing triple helices from the Polypro II-like and nonsupercoiled structures through the comparison of their thermal melting characteristics.[47] The thermal stability of the peptide-amphiphiles was studied by monitoring their ellipticity at λ = 225 nm, as a function of temperature. The melting point curves of CPA1 at different concentrations, 0.5, 0.7, and 2 mg/mL, are shown in Figure 6a, and the first derivative of mean residue ellipticity (MRE) used to indicate the melting point is represented in Figure 6b. The melting profile of CPA1 exhibited a sigmoidal feature, indicating a cooperative transition, which is typical of a triple-helical conformation. The first derivative of the melting curves gave a melting temperature (T_m) of 39 °C for 0.5 mg/mL, 39 °C for 0.7 mg/mL, and 47 °C for 2 mg/mL. The value of T_m represented the stability of the triple helix: the higher the value of T_m, the more stable the triple helix. The stability of the triple helix increased with increasing concentration, as confirmed by the increase in melting temperature. In a previous study, the melting point of collagen peptide $(GPO)_3GFOGER(GPO)_3$ at 0.5 mg/mL was found to be at 25 °C.[21] This indicates that the thermal stability of the triple helix in CPAs is higher than that of collagen peptide, which is consistent with previous reports from Fields' group that the thermal stability of the triple helix could be enhanced through amphiphilic assemblies.[37,38] The enhanced stability may be due to the flexibility of the alkyl chain and the hydrophobic interaction that drives the tails together, thus bringing the collagen peptide head groups closer. Such collagen peptide assembly results in tight alignment of the three termini, which stabilizes the triple helix.[45]

The refolding melting study was performed to investigate the refolding behavior of the triple-helical structure in the form of amphiphilic assemblies. CPA1, CPA2, and CPA3 were induced to undergo the refolding process in solution as the temperature was decreased from 80 °C to 5 °C. The unfolding and refolding melting curves of CPA1 and CPA2 at 0.7 mg/mL are shown in Figure 7. CPA3 did not possess a cooperative melting transition curve due to the absence of triple helices, as seen in Figure S3 in the Supporting Information. The symmetry between the unfolding and refolding melting curves indicates that the folding process of the triple-helical structure in CPA1 and CPA2 is reversible. For CPA1, T_m obtained from the first derivative of the refolding melting curve gives a value of 39 °C, consistent with the value obtained from the unfolding melting curve, as shown in Figure 7b. For CPA2, the T_m value of the refolding melting curve is around 42 °C, consistent with that of the unfolding melting curve, as shown in Figure 7d. The T_m of CPA2 in the unfolding and refolding process is slightly higher than that of CPA1, which may be due to more repeating units of $(GPO)_n$ and the higher stability of the triple helix in CPA2. The folding results show that the unfolded collagen-mimetic head group is almost able to completely refold into a triple-helical conformation in a short time. The ability of quick and complete refolding of CPA1 and CPA2 may be due to the tight alignment of the three collagen peptide head groups in the amphiphile, which can make the collagen head groups closer. Therefore, the triple-helical peptide gel formed by CPA1 and CPA2 nanofibers can recover quickly and completely after being denatured at high temperature.

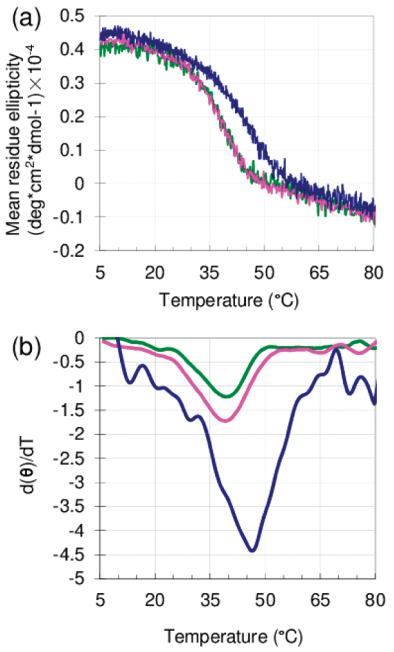

Figure 6. Unfolding melting studies of CPA1: (a) the unfolding melting curves showed cooperative transition of CPA1 at different concentrations, 0.5 mg/mL (green line), 0.7 mg/mL (pink line), and 2 mg/mL (blue line); (b) the first derivative of unfolding melting curves indicated the T_m values of 39 °C for 0.5 mg/mL, 39 °C for 0.7 mg/mL, and 47 °C for 2 mg/mL.

Cell Adhesion Assay. The bioactive motif GFOGER with the triple-helical domain of collagen has been shown to recognize and combine with several integrin receptors of $\alpha1\beta1$, $\alpha2\beta1$, $\alpha10\beta1$, and $\alpha11\beta1$.[17−20,52] Previously, we have shown that triple-helical peptides conjugated with GFOGER could specifically bind to integrin receptors of several cells.[19−21] In this study, HepG2 cells were used to examine the bioactivity of CPAs since the cells can constitutively express $\alpha1$, $\alpha2$, $\alpha6$, and $\beta1$ subunits and thus are a suitable model system in the study of bioactive motif GFOGER.[51] HepG2 cells were cultured on the surfaces of substrates coated with bovine serum albumin (BSA), collagen, CPAs (CPA1, CPA2, and CPA3), and collagen peptides (CP1, CP2, and CP3, where the sequences are $(GPO)_4GFOGER(GPO)_4$, $(GPO)_{10}$, and $(GPO)_2GFOGERGPO$, respectively). Cell adhesion to the native collagen substrate was taken as the 100%

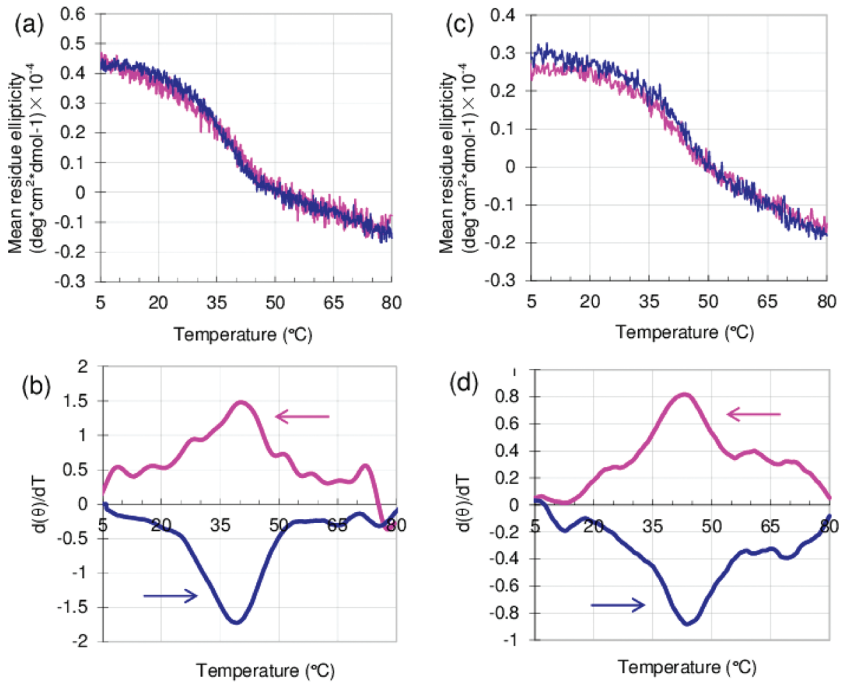

Figure 7. Melting curves of unfolding (blue line) and refolding (pink line) of CPA1 (a) and CPA2 (c) prepared at 0.7 mg/mL show that the melting transition of CPA1 and CPA2 is reversible. The rate of temperature change is 0.25 °C/min for the folding processes. The first derivative of melting curves of CPA1 (b) and CPA2 (d) shows negative and positive curves for the unfolding and refolding process, respectively. The T_m value of CPA1 is 39 °C, lower than that of CPA2, with a T_m of 42 °C. The arrows represent the direction of temperature.

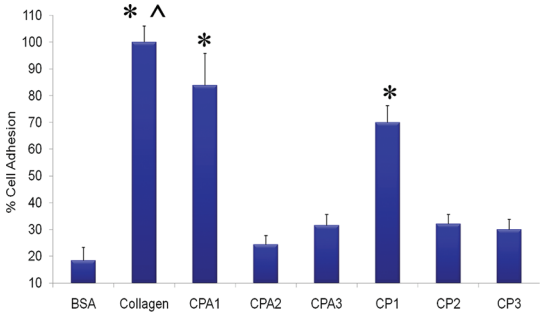

Figure 8. Adhesion of HepG2 cells as a function of surface composition: heat-denatured BSA, calf-skin collagen, CPA1, CPA2, CPA3, CP1, CP2, and CP3. Cell adhesion to collagen was used as a 100% reference level. Student's *t* test, with $p < 0.05$ for * significantly different from BSA, CPA2, CPA3, CP2, and CP3 and ^ significantly different from CPA1 and CPA2.

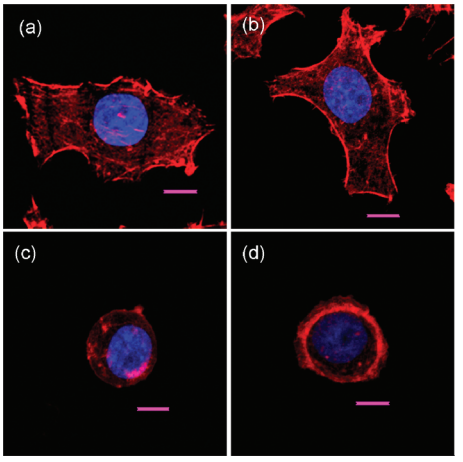

Figure 9. Cell adhesion and spreading of HepG2 cells as a function of substrates: collagen (a), CPA1 (b), CPA2 (c), and CPA3 (d). Cells were fixed and stained for actin stress fibers (red) and nuclei (blue) after being incubated in serum-free medium and examined by confocal microscopy. Scale bar is 10 μm.

reference level. It could be seen from Figure 8 that the percentages of the cell adhesion to CPA1, CPA2, CPA3, CP1, CP2, and CP3 were approximately 83%, 25%, 30%, 70%, 30%, and 28%, respectively. Cell adhesion results indicate that HepG2 cells attached on the surfaces of CPA1 and CP1 more efficiently, as compared to other surfaces. The cell-binding activity of CPA1 was slightly higher than that of CP1, indicating that the GFOGER sequence within the amphiphiles retained and even improved its cell-binding activity. The receptors on the cell membrane surface could recognize and interact with the bioactive sequence located on the periphery of the nanofiber. In addition, the absence of the GFOGER hexapeptide in CPA2 and CP2 led to a marked loss of activity and adversely affected the level of HepG2 cell adhesion. Although being conjugated with the GFOGER sequence, CPA3 and CP3 exhibited lower cell adhesion. This may be due to the absence of a triple-helical conformation of CPA3 and CP2, since the GFOGER sequence is biologically active only when present in a triple-helical conformation.[19,21] Not only thermal stability but also cell-binding ability are dependent on the triple-helical conformation.

Immunofluorescence Staining for Cell Adhesion and Spreading Study. The adhered HepG2 cells were fixed and stained for actin stress fibers and nuclei after being incubated in serum-free medium to study their cytoskeletal organization. The confocal images presented in Figure 9 showed that the HepG2 cells displayed a well-developed actin cytoskeletal structure on collagen and CPA1-coated substrates. In addition, cell adhesion and spreading were extensive on both substrates, indicating the ability of CPA1 to mimic the collagen adhesion profile. On the other hand, the actin cytoskeletal organization became less pronounced in the cells seeded on CPA2- and CPA3-coated substrates, and most HepG2 cells remained spherical. The absence of GFOGER hexapeptides or deletion of the triple-helical conformation substantially decreased HepG2 cell spreading. Cell spreading on collagen and CPA1-modified surfaces is distinctly different from the interaction between the cells and other synthetic polymers, in that the latter merely depends on the nonspecific contact between the cell membrane proteins and the functional groups of polymers.[49,50] In fact, the extensive cell spreading shown in this work may be the result of the integrin-mediated cell adhesion process. To visualize the interaction between cells and CPA1 fibers, cells cultured on the top of a thin CPA1 fiber gel were dried at the critical point and observed under SEM. SEM micrographs (see Figure S4 in the Supporting Information) show that the cells can spread well on the top of CPA1 fibers. The above results demonstrate that the self-assembled peptide nanofibers from triple-helical constructs of CPAs with the GFOGER sequence are able to promote cell adhesion and spreading, indicating the ability to biologically mimic collagen.

CONCLUSION

The present work was to synthesize and characterize novel collagen-mimetic peptide amphiphiles. It was found that CPAs could self-assemble into peptide nanofibers. Moreover, the peptide nanofibers were shown to possess a collagen-mimetic triple helix and cell adhesion ability. The results indicate that the collagen-mimetic peptide nanofibers are able to structurally and functionally mimic native collagen fibers. Compared with the artificial collagen fibers reported by other groups, collagen-mimetic peptide nanofibers synthesized in this study not only can structurally resemble the collagen-mimetic triple helix but also have functional properties of collagen such as promoting cell adhesion and cell spreading. In addition, since peptide amphiphiles are easy to synthesize and are highly versatile in displaying a broad range of chemical functionalities, there is great potential in using peptide amphiphiles to fully mimic native collagen fibrils, when more functional motifs found in collagen, such as DGEA, are incorporated into the hybrid nanofibers. In the next step, we will characterize the mechanical properties of the hydrogels that are formed by collagen-mimetic peptide nanofibers and apply this hydrogel as a scaffold for tissue engineering and regeneration.

EXPERIMENTAL SECTION

Peptide Synthesis. All peptides were synthesized in-house on an automated Multipep peptide synthesizer (Intavis, Cologne, Germany) as described previously.[19−21] Briefly, all peptides were assembled on fluorenyl-methoxy-carbonyl (Fmoc)−Gly−Wang resin (substitution level = 0.66 mmol/g resin) at a 50 μmol scale. Stepwise couplings of amino acids were accomplished using a double coupling method with 5-fold excesses of amino acids, equivalent activator reagents, benzotriazol-1-yloxytripyrrolidinophosphonium (PyBop), and two equivalents of base, *N*-methylmorpholine. The removal of Fmoc was completed using 20% piperidine in dimethylformamide (DMF). Cycles of deprotection, washing, double coupling, and washing were repeated until the desired peptide sequence was achieved. After the peptide portion of the molecule was prepared, the resin was removed from the automated synthesizer and the N-terminus was capped with a fatty acid containing 16 carbon atoms. The alkylation reaction was accomplished using five equivalents of the fatty acid, five equivalents of PyBop, and two equivalents of base, *N*-methylmorpholine. The reaction was allowed to proceed for at least 6 h, after which it was monitored by ninhydrin. The alkylation reaction was repeated until the ninhydrin test was negative. Then the dried peptidyl resin was cleaved by a cocktail solution composed of 95% trifluoroacetic acid, 2.5% deionized water, and 2.5% triethylsilane (v/v). The purity of all peptides was greater than 90% according to analytical reverse phase HPLC and matrix-assisted laser desorption/ionization time-of-flight (MALDI-TOF) mass spectroscopy on a Bruker Auto-Flex II MALDI-TOF mass spectroscope (Bruker, Bremen, Germany).

Base-Induced Self-Assembly of CPAs. Samples of 1 mg/mL concentration were dissolved in water and stored at 4 °C at least 2 d prior to base-induced assembly. The samples were placed in a small glass vial with an open top. This vial and a second open top vial filled with NH_4OH were placed together in a sealed glass chamber, where the NH_4OH vapor was allowed to slowly diffuse into the PA solution.

Transmission Electron Microscopy. TEM images were taken on a JEOL JEM 2010 operating at 200 kV accelerating voltage. The samples were prepared on a holey carbon copper grid. Negative staining was carried out with 1 wt % phosphotungstic acid in water. TEM grids were prepared by casting 10 μL of PAs onto the carbon side of the grid, followed by wicking off the excess moisture with filter paper after 1 min. Negative staining was then performed by placing the grid carbon-side down on a droplet of filtered phosphotungstic acid solution for 30 s. The TEM samples were air-dried for at least 3 h before imaging. In all cases, electron microscopy was performed at an acceleration voltage of 200 kV.

Circular Dichroism Spectroscopy. Circular dichroism measurements were performed on a J-810 spectropolarimeter (Jasco, Great Dunmow, Essex, UK) using a 1 mm quartz cuvette (Hellma, Germany). All samples were prepared and stored at 4 °C for at least 3 d before the test, to allow for proper equilibration of the triple-helical conformation. A volumn of 200 μL of samples was used for each measurement. The CD spectra were obtained

using continuous wavelength scans (average of eight scans) from 260 nm to 180 nm, at a scan speed of 50 nm/min.

Melting Studies. Melting studies were performed on a J-810 spectropolarimeter (Jasco, Great Dunmow, Essex, UK) using a 1 mm quartz cuvette (Hellma, Germany). Melting point curves were obtained by recording the ellipticity at 225 nm, while the temperature was continuously increased between 5 and 80 °C, at a rate of 0.25 °C/min. For samples exhibiting sigmoidal melting curves, the reflection point in the transition region (first derivative) is defined as the melting temperature (T_m). Peptides and peptide−amphiphiles were prepared and stored at 4 °C at least 24 h prior to the experiments. In the refolding studies, the samples were kept at 80 °C for 30 min prior to the experiments. The refolding melting point curves were obtained by recording the ellipticity at 225 nm while the temperature was continuously decreased from 80 °C to 5 °C at a rate of 0.25 °C/min.

Cell Adhesion Assay. Nunclon Delta TC Microwell plates were coated with one thin layer of collagen, CPA1, CPA2, CPA3, CP1, CP2, and CP3. In the blank group, the wells of the plate were coated with heat-denatured BSA (Sigma-Aldrich). Before culturing the cells, the CPA gels were washed with phosphate-buffered saline (PBS) solution five times and then were incubated overnight in PBS solution. After this treatment, the pH was reduced to 7−8, and there was no apparent damage to the structure of the peptide gels. Then a volume of 100 μL of HepG2 cell suspension in serum-free Dulbecco's modified Eagle medium (10×10^5 cells/mL) was added, and the mixture incubated for 1 h at 20 °C.

Unattached cells were washed away with PBS twice. Adhered cells were measured using a total deoxyribonucleic acid (DNA) quantification assay (Hoechst 33258, Sigma-Aldrich). Briefly, the cells were lyzed using three freeze−thaw cycles in ultrapure water, and the cell lysates were mixed with 2 mg/mL bisbenzimide in 10 mM TrisHCl (pH 7.4), 1 mM ethylenediaminetetraacetic acid (EDTA), and 0.2 M sodium chloride (NaCl) fluorescence assay buffer and were incubated in the dark for 30 min. The fluorescence was read on a microplate reader (Tecan Infinite M200) using an excitation wavelength of 360 nm and an emission wavelength of 465 nm. Assays were conducted in triplicate, and the data were expressed as means ± standard deviations (SDs). BSA-coated wells were used as a baseline reference level, and the adhesion to the collagen-coated well was used as a 100% reference level.

Immunofluorescence Staining. Coverslips were coated with one thin layer of either collagen, CPA1, CPA2, or CPA3. Before culturing the cells, the coverslips were washed using PBS solution five times and incubated overnight. Then HepG2 cells were allowed to adhere on the coverslips at a density of 280 cells/mm^2 in serum-free medium for 3 h. Attached cells were fixed in cold 3.7% formaldehyde for 5 min, permeabilized with 0.1% Triton X-100 for 5 min, and blocked in blocking buffer (1% BSA in PBS) for 0.5 h. The cell actin cytoskeleton and cell nucleus were stained by incubating the cells with phalloidin−tetramethylrhodamine isothiocyanate (Sigma−Aldrich) (1:1000 dilution in PBS) for 1 h and Hoechst (Sigma-Aldrich) (dilution 1:10000) for 5 min.

Statistical Analysis. The data are presented as means ± SDs. The statistical analysis of the data was done using Student's *t* test. A 95% confidence level was considered significant.

Acknowledgment. We acknowledge the support by the National University of Singapore (NUS) through grant R279000328112. The research scholarship for J.L. is funded by NUS.

Supporting Information Available: Figures S1 to S4. This information is available free of charge *via* the Internet at http://pubs.acs.org

REFERENCES AND NOTES

1. Zhao, X.; Zhang, S. Molecular Designer Self-Assembling Peptides. *Chem. Soc. Rev.* **2006**, *35*, 1105–1110.
2. Shoulders, M. D.; Raines, R. T. Collagen Structure and Stability. *Annu. Rev. Biochem.* **2009**, *78*, 929–958.
3. Fernandes, H.; Moroni, L.; Van Blitterswijk, C; De Boer, J. Extracellular Matrix and Tissue Engineering Applications. *J. Mater. Chem.* **2009**, *19*, 5474–5484.
4. Brodsky, B.; Ramshaw, J. A. The Collagen Triple-Helix Structure. *Matrix Biol.* **1997**, *15*, 545–554.
5. Kadler, K. E.; Hill, A.; Canty-Laird, E. G. Collagen Fibrillogenesis: Fibronectin, Integrins, and Minor Collagens as Organizers and Nucleators. *Curr. Opin. Cell Biol.* **2008**, *20*, 495–501.
6. Perumal, S.; Antipova, O.; Orgel, J. P. Collagen Fibril Architecture, Domain Organization, and Triple-Helical Conformation Govern Its Proteolysis. *Proc. Natl. Acad. Sci. U. S. A.* **2008**, *105*, 2824–2829.
7. Zhang, W. M.; Käpylä, J.; Puranen, J. S.; Knight, C. G.; Tiger, C. F.; Pentikäinen, O. T.; Johnson, M. S.; Farndale, R. W.; Heino, J.; Gullberg, D. $\alpha 11\beta 1$ Integrin Recognizes the GFOGER Sequence in Interstitial Collagens. *J. Biol. Chem.* **2003**, *278*, 7270–7277.
8. Velling, T.; Kusche-Gullberg, M.; Sejersen, T.; Gullberg, D. cDNA Cloning and Chromosomal Localization of Human $\alpha 11$ Integrin. A Collagen-Binding, I Domain-Containing, $\beta 1$-Associated Integrin α-Chain Present in Muscle Tissues. *J. Biol. Chem.* **1999**, *274*, 25735–25742.
9. Camper, L.; Hellman, U.; Lundgren-Åkerlund, E. Isolation, Cloning, and Sequence Analysis of the Integrin Subunit $\alpha 10$, a $\beta 1$-Associated Collagen Binding Integrin Expressed on Chondrocytes. *J. Biol. Chem.* **1998**, *273*, 20383–20389.
10. Kramer, R. H.; Marks, N. Identification of Integrin Collagen Receptors on Human Melanoma Cells. *J. Biol. Chem.* **1989**, *264*, 4684–4688.
11. Fields, G. The Collagen Triple-Helix: Correlation of Conformation with Biological Activities. *Connect. Tissue Res.* **1995**, *31*, 235–243.
12. Hynes, R. O. Integrins: Versatility, Modulation, and Signaling in Cell Adhesion. *Cell* **1992**, *69*, 11–25.
13. Ruoslahti, E.; Reed, J. C. Anchorage Dependence, Integrins, and Apoptosis. *Cell* **1994**, *77*, 477–478.
14. Holmgren, S. K.; Bretscher, L. E.; Taylor, K. M.; Raines, R. T. A Hyperstable Collagen Mimic. *Chem. Biol.* **1999**, *6*, 63–70.
15. Feng, Y.; Melacini, G.; Goodman, M. Collagen-Based Structures Containing the Peptoid Residue N-Isobutylglycine (Nleu): Synthesis and Biophysical Studies of Gly-Nleu-Pro Sequences by Circular Dichroism and Optical Rotation. *Biochemistry* **1997**, *36*, 8716–8724.
16. Feng, Y.; Melacini, G.; Taulane, J. P.; Goodman, M. Collagen-Based Structures Containing the Peptoid Residue N-Isobutylglycine (Nleu): Synthesis and Biophysical Studies of Gly-Pro-Nleu Sequences by Circular Dichroism, Ultraviolet Absorbance, and Optical Rotation. *Biopolymers* **1996**, *39*, 859–872.
17. Knight, C. G.; Morton, L. F.; Peachey, A. R.; Tuckwell, D. S.; Farndale, R. W.; Barnes, M. J. The Collagen-Binding A-Domains of Integrins $\alpha 1/\beta 1$ and $\alpha 2/\beta 1$ Recognize the Same Specific Amino Acid Sequence, GFOGER, in Native (Triple-Helical) Collagens. *J. Biol. Chem.* **2000**, *275*, 35–40.
18. Knight, C. G.; Morton, L. F.; Onley, D. J.; Peachey, A. R.; Messent, A. J.; Smethurst, P. A.; Tuckwell, D. S.; Farndale, R. W.; Barnes, M. J. Identification in Collagen Type I of an Integrin $\alpha 2\beta 1$-Binding Site Containing an Essential GER Sequence. *J. Biol. Chem.* **1998**, *273*, 33287–33294.
19. Khew, S. T.; Tong, Y. W. The Specific Recognition of a Cell Binding Sequence Derived from Type I Collagen by Hep3B and L929 Cells. *Biomacromolecules* **2007**, *8*, 3153–3161.
20. Khew, S. T.; Yang, Q. J.; Tong, Y. W. Enzymatically Cross-linked Collagen-Mimetic Dendrimers That Promote Integrin-Targeted Cell Adhesion. *Biomaterials* **2008**, *29*, 3034–3045.
21. Khew, S. T.; Zhu, X. H.; Tong, Y. W. An Integrin-Specific Collagen-Mimetic Peptide Approach for Optimizing Hep3B Liver Cell Adhesion, Proliferation, and Cellular Functions. *Tissue Eng.* **2007**, *13*, 2451–2463.
22. Reyes, C. D.; García, A. J. $\alpha 2\beta 1$ Integrin-Specific Collagen-Mimetic Surfaces Supporting Osteoblastic Differentiation. *J. Biomed. Mater. Res., Part A* **2004**, *69*, 591–600.

23. Reyes, C. D.; García, A. J. Engineering Integrin-Specific Surfaces with a Triple-Helical Collagen-Mimetic Peptide. *J. Biomed. Mater. Res., Part A* **2003**, *65*, 511–523.
24. Koide, T.; Homma, D. L.; Asada, S.; Kitagawa, K. Self-Complementary Peptides for the Formation of Collagen-like Triple Helical Supramolecules. *Bioorg. Med. Chem. Lett.* **2005**, *15*, 5230–5233.
25. Kotch, F. W.; Raines, R. T. Self-Assembly of Synthetic Collagen Triple Helices. *Proc. Natl. Acad. Sci. U. S. A.* **2006**, *103*, 3028–3033.
26. Cejas, M. A.; Kinney, W. A.; Chen, C.; Leo, G. C.; Tounge, B. A.; Vinter, J. G.; Joshi, P. P.; Maryanoff, B. E. Collagen-Related Peptides: Self-Assembly of Short, Single Strands into a Functional Biomaterial of Micrometer Scale. *J. Am. Chem. Soc.* **2007**, *129*, 2202–2203.
27. Przybyla, D. E.; Chmielewski, J. Metal-Triggered Radial Self-Assembly of Collagen Peptide Fibers. *J. Am. Chem. Soc.* **2008**, *130*, 12610–12611.
28. Rele, S.; Song, Y.; Apkarian, R. P.; Qu, Z.; Conticello, V. P.; Chaikof, E. L. *D*-Periodic Collagen-Mimetic Microfibers. *J. Am. Chem. Soc.* **2007**, *129*, 14780–14787.
29. Hartgerink, J. D.; Beniash, E.; Stupp, S. I. Peptide-Amphiphile Nanofibers: a Versatile Scaffold for the Preparation of Self-Assembling Materials. *Proc. Natl. Acad. Sci. U. S. A.* **2002**, *99*, 5133–5138.
30. Hartgerink, J. D.; Beniash, E.; Stupp, S. I. Self-Assembly and Mineralization of Peptide-Amphiphile Nanofibers. *Science* **2001**, *294*, 1684–1688.
31. Paramonov, S. E.; Jun, H. W.; Hartgerink, J. D. Self-Assembly of Peptide-Amphiphile Nanofibers: the Roles of Hydrogen Bonding and Amphiphilic Packing. *J. Am. Chem. Soc.* **2006**, *128*, 7291–7298.
32. Jun, H. W.; Paramonov, S. E.; Hartgerink, J. D. Biomimetic Self-Assembled Nanofibers. *Soft Matter* **2006**, *2*, 177–181.
33. Niece, K. L.; Hartgerink, J. D.; Donners, J. J.; Stupp, S. I. Self-Assembly Combining Two Bioactive Peptide-Amphiphile Molecules into Nanofibers by Electrostatic Attraction. *J. Am. Chem. Soc.* **2003**, *125*, 7146–7147.
34. Silva, G. A.; Czeisler, C.; Niece, K. C.; Beniash, E.; Harrington, D. A.; Kessler, J. A.; Stupp, S. I. Selective Differentiation of Neural Progenitor Cells by High-Epitope Density Nanofibers. *Science* **2004**, *303*, 1352–1355.
35. Webber, M. J.; Tongers, J.; Renault, M. A.; Roncalli, J. G.; Losordo, D. W.; Stupp, S. I. Development of Bioactive Peptide Amphiphiles for Therapeutic Cell Delivery. *Acta Biomater.* **2010**, *6*, 3–11.
36. Yu, Y. C.; Tirrell, M.; Fields, G. B. Minimal Lipidation Stabilizes Protein-Like Molecular Architecture. *J. Am. Chem. Soc.* **1998**, *120*, 9979–9987.
37. Yu., Y. C.; Pakalns, T.; Dori, Y.; Mccarthy, J. B.; Tirrell, M.; Fields, G. B. Construction of Biologically Active Protein Molecular Architecture Using Self-Assembling Peptide-Amphiphiles. *Methods Enzymol.* **1997**, *289*, 571–587.
38. Fields, G. B.; Lauer, J. L.; Dori, Y.; Forns, P.; Yu, Y. C.; Tirrell, M. Proteinlike Molecular Architecture: Biomaterial Applications for Inducing Cellular Receptor Binding and Signal Transduction. *Biopolymers* **1998**, *47*, 143–151.
39. Yu, Y. C.; Roontga, V.; Daragan, V. A.; Mayo, K. H.; Tirrell, M.; Fields, G. B. Structure and Dynamics of Peptide-Amphiphiles Incorporating Triple-Helical Proteinlike Molecular Architecture. *Biochemistry* **1999**, *38*, 1659–1668.
40. Fields, G. B. Synthesis and Biological Applications of Collagen-Model Triple-Helical Peptides. *Org. Biomol. Chem.* **2010**, *8*, 1237–1258.
41. Yu, Y. C.; Berndt, P.; Tirrell, M.; Fields, G. Self-Assembling Amphiphiles for Construction of Protein Molecular Architecture. *J. Am. Chem. Soc.* **1996**, *118*, 12515–12520.
42. Sakakibara, S.; Kishida, Y.; Okuyama, K.; Tanaka, N.; Ashida, T.; Kakudo, M. Single Crystals of $(Pro\text{-}Pro\text{-}Gly)_{10}$, a Synthetic Polypeptide Model of Collagen. *J. Mol. Biol.* **1972**, *65*, 371–373.
43. Brown, F. R., 3rd; Di Corato, A.; Lorenzi, G. D.; Blout, E. R. Synthesis and Structural Studies of Two Collagen Analogues: Poly (l-Prolyl-l-Seryl-Glycyl) and Poly (l-Prolyl-l-Alanyl-Glycyl). *J. Mol. Biol.* **1972**, *63*, 85–99.
44. Rippon, W. B.; Walton, A. G. Optical Properties of the Polyglycine II Helix. *Biopolymers* **1971**, *10*, 1207–1212.
45. Bella, J.; Eaton, M.; Brodsky, B.; Berman, H. M. Crystal and Molecular Structure of a Collagen-Like Peptide at 1.9 Å Resolution. *Science* **1994**, *266*, 75–81.
46. Bella, J.; Brodsky, B.; Berman, H. M. Hydration Structure of a Collagen Peptide. *Structure* **1995**, *3*, 893–906.
47. Jefferson, E. A.; Locardi, E.; Goodman, M. Incorporation of Achiral Peptoid-Based Trimeric Sequences into Collagen Mimetics. *J. Am. Chem. Soc.* **1998**, *120*, 7420–7428.
48. Gore, T.; Dori, Y.; Talmon, Y.; Tirrell, M.; Bianco-Peled, H. Self-Assembly of Model Collagen Peptide Amphiphiles. *Langmuir* **2001**, *17*, 5352–5360.
49. Bačáková, L.; Mareš, V.; Bottone, M. G.; Pellicciari, C.; Lisá, V.; Švorčík, V. Fluorine Ion-Implanted Polystyrene Improves Growth and Viability of Vascular Smooth Muscle Cells in Culture. *J. Biomed. Mater. Res.* **2000**, *49*, 369–379.
50. Bačáková, L.; Mareš, V.; Lisá, V.; Švorčík, V. Molecular Mechanisms of Improved Adhesion and Growth of an Endothelial Cell line Cultured on Polystyrene Implanted with Fluorine Ions. *Biomaterials* **2000**, *21*, 1173–1179.
51. Nejjari, M.; Hafdi, Z.; Dumortier, J.; Bringuier, A. F.; Feldmann, G.; Scoazec, J. Y. $\alpha 6\beta 1$ Integrin Expression in Hepatocarcinoma Cells: Regulation and Role in Cell Adhesion and Migration. *Int. J. Cancer* **1999**, *83*, 518–525.
52. Janet, A.; Martin, H. Cell-Matrix Interaction. In *Encyclopedia of Biological Chemistry*; William, L.; M. Daniel, L., Eds.; Academic Press: New York, 2004; pp 362−366.